processes

MDPI

Article

Characterization, Expression Profiling, and Functional Analyses of a 4CL-Like Gene of *Populus trichocarpa*

Hui Wei †, Chen Xu †, Ali Movahedi †, Weibo Sun † and Qiang Zhuge *

Co-Innovation Center for Sustainable Forestry in Southern China, Key Laboratory of Forest Genetics and Biotechnology, Ministry of Education, College of Biology and the Environment, Nanjing Forestry University, Nanjing 210037, China; 15850682752@163.com (H.W.); xuchenidea@hotmail.com (C.X.); ali_movahedi@njfu.edu.cn (A.M.); cz851115@126.com (W.S.)

* Correspondence: qzhuge@njfu.edu.cn; Tel./Fax: +86-25-85428701

† These authors contributed equally to this work.

Received: 2 December 2018; Accepted: 11 January 2019; Published: 16 January 2019

Abstract: Adenosine 5′-monophosphate (AMP) (adenylate)-forming acetyl-CoA synthetase (ACS) catalyzes the formation of acetyl-coenzyme A (CoA), and the ACS family is closely related to the 4-coumarate CoA ligase (4CL) family. In this study, a 4CL-like gene was cloned from *Populus trichocarpa* and named Pt4CL-like. Characterization of Pt4CL-like, using bioinformatics, showed that it contained box I and box II domains at the end of the C-terminal sequence, and there is a characteristic sequence of ACS, namely, peroxisome-targeting sequence (PTS). Real-time PCR results showed that the 4CL-like gene was expressed in all tissues tested, and was highly expressed in the stems. A denaturation and renaturation process was conducted, and the recombinant *Pt4CL-like* protein was purified through HisTrap^{TM} high performance affinity chromatography. It showed *Pt4CL-like* protein did not catalyze substrates of 4CL, but could significantly catalyzed sodium acetate. These results indicate that *Pt4CL-like* protein belongs to the ACS family, providing a theoretical basis for further analysis and comparison of the functions of adenylate-forming enzymes and 4CL family.

Keywords: ACS; CL; 4CL-like; PTS; box I domain; box II domain; *Populus trichocarpa*

1. Introduction

The genome of *Populus trichocarpa* contains a large number of genes encoding carboxylic acid-activating enzymes, including long-chain fatty acyl-coenzyme A (CoA) synthetases, 4-coumarate: CoA ligases (4CL), and 4CL-like proteins of unknown biochemical function. The adenylate-forming enzyme superfamily is divided into several subfamilies according to substrate, including the acetyl coenzyme ligase, short-chain coenzyme ligase, long-chain coenzyme ligase, coumaric acid coenzyme ligase, luciferase, and adenylate domain nonribosomal peptide synthetase subfamilies [1]. In addition, adenylate-forming enzymes contain the highly conserved Adenosine 5′-monophosphate (AMP)-binding and Adenosine triphosphate (ATP)-dependent domains, which indicates the specific functions of enzymes. Adenylate-forming enzymes utilize a two-step mechanism. In the first step, ACS combines acetate with ATP to form the intermediate acetyl adenylate (AcAMP), referred to as adenylate, with concomitant release of pyrophosphate. The second step is characterized by the formation of acyl-CoA and AMP, causing CoA and AMP to be released [2–4].

4CL plays an important role in the biosynthesis of lignin. It can convert various numbers of cinnamic acid derivatives, including coumarate, caffeate, and ferulate, into coenzyme A (CoA)-linked intermediates, and these activated phenolic acids serve as precursors for the biosynthesis of lignin [5,6]. Previous studies have shown that 4CL enzymes expressed in higher plants have multiple isoforms, and they often have distinct catalytic properties and expression profiles that regulate CoA ligation

fluxes in specific plant tissues. For example, the *4CL* genes of *Arabidopsis thaliana*, *At4CL1 and At4CL2*, are mainly expressed in lignifying cells and are involved in the formation of lignin, whereas *At4CL3* is expressed in a broad range of cell types and is involved in the flavonoid biosynthesis pathway. Meanwhile, *At4CL4* is hardly detectable and promotes the formation of lignin [7,8]. In accordance with *Arabidopsis thaliana*, *Populus trichocarpa* also has multiple isoforms. *Ptr4CL3* and *Ptr4CL5* have high transcriptional levels in differentiating xylem. Ptr4CL3 can regulate the β-coumaric acid and caffeic acid CoA ligation pathways, while Ptr4CL5 regulates only the caffeic acid pathway, and caffeic acid modulates the CoA ligation flux for monolignol biosynthesis [9–11].

With further research and complete sequencing of the *Arabidopsis* genome, researchers have gradually uncovered eight genes in *Arabidopsis* that are highly similar to the 4CL conserved domain containing box I and box II, which can be classified as 4CL-like genes [12–14]. However, these genes have no corresponding 4CL substrates (β-coumaric acid, caffeic acid, ferulic acid, 5-hydroxyferulic acid, and erucic acid), and have no direct relationship with the synthesis of lignin or flavonoid compounds in terms of expression [14]. Although most 4CL-like genes have unknown functions, several have specific biochemical roles. For example, the At1g20510 protein exhibits cyclopentane-1-octanoic acid (OPC-8) CoA ligase activity, which is an essential step in jasmonate biosynthesis [15]. These results show that 4CL-like genes may belong to the acetyl-CoA synthetase (ACS) family [16]. Compared to the herb *Arabidopsis thaliana*, the poplar tree has a larger genome, in which more 4CL-like genes have been cloned and characterized. It has been predicted that the total poplar genome contains 17 4CL genes [10]. Five of these genes have been recognized as 4CL genes, while the others have not clearly been identified, but generally do not show the catalytic activity characteristic of 4CL [17]. Peroxisome-targeting sequence 1 (PTS1) is generally in the C-terminal region of the majority of 4CL-like enzymes and targets peroxisome [1,18]. PTS1 is characterized by a sequence consisting of three amino acid residues, and is considered a characteristic sequence of peroxisomes. Therefore, the suspected 4CL-like proteins with a PTS1 sequence are highly likely to have CoA ligase activity, rather than acting as a true 4CL. Recently, studies have shown that the fused PTS1 sequences of these proteins participate in the jasmonic acid synthesis pathway, playing the role of CoA ligase [15,18]. However, due to the high homology sequence in the supergene family of adenylate synthase, it is very difficult to identify this using gene sequence analyses, therefore, it is necessary to use different substrates for enzymatic reactions to identify the function of 4CL-like protein. Based on previous findings, the characterization, expression profiling, and function of 4CL-like genes should be investigated.

In this study, we performed molecular cloning, characterization, and functional analyses of the 4CL-like gene of *P. trichocarpa*. We investigated the functions of this enzyme and its expression patterns in different tissues and under various abiotic stresses. The results show that the 4CL-like gene belongs to the ACS family. In addition, the 4CL-like gene was expressed in roots, stems, leaves, and petioles, but the expression level are different. In addition, the results showed high transcriptional levels in the upper stem region and low expression in roots. Moreover, the *Pt4CL-like* gene can be induced with 200 mM NaCl, 200 μM abscisic acid, 2 mM H_2O_2, 4 °C cold stress, or 10% PEG_{6000}.

2. Materials and Methods

2.1. Materials

Three-month-old seedlings of *P. trichocarpa* grown on sterile half-strength Murashige and Skoog (MS) medium (pH 5.8). Total RNA was extracted from *P. trichocarpa* plants. *Escherichia coli* strains, including Top10 cells and BL21 (DE3) cells, were utilized. Top10 cells were employed in cloning and propagation, and BL21 (DE3) cells were used for protein expression. PCR cleanup kits were purchased from Takara Biotechnology Co., Ltd. (Dalian, China). Primer synthesis and DNA sequencing were performed by Invitrogen Biotechnology Company (Shanghai, China).

2.2. RNA Isolation and cDNA Synthesis

RNAs were extracted from different tissue parts using the Biomiga Miniprep kit, according to the manufacturer's instruction, and cDNA was synthesized with 5× PrimeScript Master Mix (Takara, Dalian, China), according to the manufacturer's instruction.

2.3. Cloning of the Open Reading Frame (ORF) and Rapid Amplification of cDNA Ends (RACE)

The full-length sequence, including the 3′- and 5′-untranslated regions of the 4CL-like gene, was achieved using rapid amplification of cDNA ends (RACE). To identify the 5′-untranslated regions, reverse primers 5′ GSP1 and 5′ GSP2 designed according to the homology, and the forward primers universal primer mix (UPM) and nest universal primer mix (NUP) were used to carry out the PCR. To achieve the 3′-untranslated regions, the forward primers 3′ GSP1 and 3′ GSP2 designed based on the homology sequences, and the 3′-outer and 3′-inner reverse primers were adapted to execute the PCR. The above PCR products were ligated into the PEASY-T3 vector (pEASY-T3 cloning kit, Beijing, China) and sequenced. The opening reading frame of the cDNA encoding the 4CL-like gene was amplified via PCR. The primers used are shown in Table 1. Then, PCR was performed in a volume of 50 µL containing 2.0 µL template cDNA, 1.5 µL each of the forward and reverse primers, 5.0 µL 10× PCR buffer (Mg2+ plus), 4 µL dNTPs, and 0.5 µL rTaq DNA polymerase (Takara Biotechnology Co., Ltd., Dalian, China). The reaction was performed as follows: 95 °C for 7 min, 35 cycles of 95 °C for 50 s, 58 °C for 50 s, and 72 °C for 2 min and, finally, 72 °C for 10 min. Next, the PCR product was purified and cloned into the PEASY-T3 vector, and then transformed into *E. coli* Trans TI. According to the results of a color reaction system using X-Gal and isopropyl β-D-1-thiogalactopyranoside (IPTG), the positive clones were isolated and sequenced (Invitrogen). The ExPASy online tool (http://www.expasy.org/) was used to analyze the nucleotide sequence, and deduce the amino acid sequence, and open reading frame (ORF) of the 4CL-like gene. The molecular weights (MWs) and predicted isoelectric points (pIs) were also calculated using ExPASy online. The Scanprosite search function of the PROSITE database in ExPASy online was used to predict the structural and functional domains of 4CL-like protein. Also, the PORTER server (http://distil.ucd.ie/porter/) at Dublin University and the SWISS-MODEL server (http://www.expasy.org/swissmod/SWISS-MODEL.html) were used to analyze the advanced structure of proteins. MEGA software (ver. 5.0, MEGA, Arizona State University, USA) was used to analyze the multiple alignment and construct a phylogenetic tree of 4CL-like genes.

Table 1. Gene-specific primers.

Primer	Direction	Nucleotide Sequence (5′–3′)
Pt4CL-like F	Forward	ATGGCAGACAACAACAACCTC
Pt4CL-like R	Reverse	TCAGAGCTTGGAGGTTGCG
3′GSP-1-*Pt4CL-like*	Forward	TATCCAGGGGTTACGATTTT
3′Outer	Reverse	TACCGTCGTTCCACTAGTGATTT
3′GSP-2-*Pt4CL-like*	Forward	GCAGGTCGGGCAGTTCC
3′Inter	Reverse	CGCGGATCCTCCACTAGTGATTTCACTATAGG
UPM	Forward	CTAATACGACTCACTATAGGGCAAGCAAGCAGTGGTATCAAACGCAGAGT (long) CTAATACGACTCACTATAGGGC (short)
5′GSP-1-*Pt4CL-like*	Reverse	AGGAAACGGTATTACAGCAG
NUP	Forward	AAGCAGTGGTATCAACGCAGAGT
5′GSP-2-*Pt4CL-like*	Reverse	ATCCTTTCGGAGAATCTT
q-*Pt4CL-like*	Forward	CTGCACTGTGTTTCCGTTTC
q-*Pt4CL-like*	Reverse	GACGCTATTGACATGAGCAG
q-*actin*	Forward	TAACGCTTTGCTGGTGAACC
q-*actin*	Reverse	GCAATGCCTCTAGTTCTGCC
PET-*Pt4CL-like*	Forward	ATAAGAATGCGGCCCTCATGGCAGACAACAACAACCTC
PET-*Pt4CL-like*	Reverse	GGAATTCCATATGTCAGAGCTTGGAGGTTGCG

2.4. Vector Construction and Heterologous Expression

The ORF of *Pt4CL-like* and the restriction site was amplified via PCR (Table 1). Then, the PCR product was cloned into pET28a via two restriction sites (*Not*I and *Nde*I). The vector pET28a-*Pt4CL-like*

was transformed into *Escherichia coli* BL21 (DE3) cells. *E. coli* BL21 (DE3)/pET28a-*Pt4CL-like* was grown overnight in 3 mL Luria-Bertani broth (LB) medium containing 50 μg/mL kanamycin, and transferred into 1 L LB medium containing kanamycin. This 1 L LB was incubated at 37 °C with 220 rpm. When the optical density (OD) at 600 nm was 0.6, 1 mM IPTG was added to l L LB to induce expression and with incubation at 37 °C, 220 rpm for 4 h. After expression was induced, the sediment was pelleted, and the bacteria were collected. The uninduced and induced solutions were analyzed via 12% sodium dodecyl sulfate polyacrylamide gel electrophoresis (SDS-PAGE, Solarbio Co., Beijing, China). Subsequently, the collected bacteria were suspended and mixed with 100 mL bacterial lysis buffer (20 mM Tris-base (Solarbio Co., Beijing, China), 500 mM NaCl (Solarbio Co., Beijing, China), and 20 mM imidazole (Solarbio Co., Beijing, China). Next, the cell suspension was sonicated on ice using 2 bursts and 6 s cooling periods for 10 min using an ultrasonic cell disruptor. The lysate was centrifuged at 4 °C, 14,000× *g* for 15 min. The precipitate and supernatant were analyzed via 12% SDS-PAGE.

2.5. Denaturation and Renaturation of Recombinant Protein

Most of the target protein remained in the form of inclusion bodies in the precipitate after sonication, and no target protein was detected in the supernatant through 12% SDS-PAGE. Therefore, the denaturation and renaturation technique was used to achieve target proteins with biological activity. The process of denaturation was carried out as follows: First, inclusion body washing solution 1 (2 M urea, 20 mM Tris, 1 mM ethylenediaminetetraacetic acid (EDTA), 1 M NaCl, and 1% Triton X-100, pH 8.5) was used to wash the collected precipitate three times. Subsequently, the collected solution was centrifuged, and precipitate was washed two times with inclusion body washing solution 2 (4 M urea, 20 mM Tris, 1 mM EDTA, 1 M NaCl, and 1% Triton X-100, pH 8.5) and the collected solution was centrifuged at 13,000 rpm for 20 min at 4 °C. Then the precipitate was washed once with inclusion body washing solution 3 (6 M urea, 20 mM Tris, 1 mM EDTA, 1 M NaCl, and 1% Triton X-100, pH 8.5). Finally, the precipitate was collected and dissolved in inclusion body dissolving solution 4 (8 M urea, 20 mM Tris, 1 mM EDTA, 1 M NaCl, and 1% Triton X-100, pH 8.5). The collected denaturation solution was stored for 48 h at 4 °C, and then centrifuged at 13,000 rpm for 20 min at 4 °C. The inclusion bodies in the dissolving solution were added dropwise to 20 mM Tris (pH 8.5). The process of renaturation is more complex and takes longer, as precipitation of protein from the solution does not occur during the process of renaturation. Renaturation buffer (4–0.5 M urea, 0.5 M NaCl, 10 mM Tris, 0.5 mM EDTA, 1 mM L-arginine, 1 mM reduced L-glutathione, 0.2 mM oxidized L-glutathione, and 5 mM DL-Dithiothreitol (DTT), pH 8.5) was added sequentially around the denatured protein contained in the dialysis bag, and dialyzed overnight in a 4 °C chromatography cabinet. During dialysis, the concentration was reduced and binding buffer (20 mM Tris-base, 500 mM NaCl, and 20 mM imidazole) was used as the final dialysis buffer.

2.6. Purification of the Recombinant Pt4CL-Like and Western Blotting

The regenerated solution was applied to a Ni^{2+}-NTA-chelating column equilibrated with Ni-NTA binding buffer (20 mM Tris-base, 500 mM NaCl, and 20 mM imidazole). After washing with Ni-NTA washing buffer until the baseline absorbance was reached, the column was washed with 250 mM imidazole in buffer (20 mM Tris-HCl and 500 mM NaCl, pH 8.5) at a flow rate of 1 mL/min. Fractions were collected and analyzed with 12% SDS-PAGE. Following overnight dialysis at 4 °C with phosphate-buffered saline (PBS), the protein was lyophilized. The purified proteins separated by SDS-PAGE were transferred to a polyvinylidene difluoride (PVDF) membrane (Solarbio Co., Beijing, China). The membrane was incubated with horseradish peroxidase (HRP)-conjugated rabbit anti-His Tag antibody IgG (Zhongshan Biotechnique, Beijing, China) at 4 °C overnight.

2.7. Enzymatic Activity of Pt4CL-Like

4CL activity was determined through the spectrophotometric assay described by Knobloch et al. The system for the reaction of the enzyme activity assay included 2 μg of purified protein, 5 mM

ATP, 0.33 mM CoA, 500 mM Tris-HCl (pH 7.8), and 25 mM $MgCl_2$. After the reaction mixtures were mixed, they were incubated at room temperature for 10 min, and the absorbances of 4-coumaroyl-CoA, caffeoyl-CoA, and feruloyl-CoA were monitored by spectrophotometry at wavelengths of 333, 363, and 345 nm, respectively [14,19]. The reaction mixture contained 12.5 µL 0.2 M $MgCl_2$, 50 µL 0.1 M ATP, 30 µL 20 mM CoA, 30 µL 0.2 M sodium acetate, 50 µL hydroxylamine solution, and a specific amount of protein. The reaction was initiated using ATP and carried out at 37 °C for 10 min. A volume of 1 mL ferric chloride reagent (0.5 mol·L^{-1} ferric chloride, 0.6 mol·L^{-1} hydrochloric acid) was added to stop the reaction. Next, the tubes were centrifuged at 12,000× *g* for 2 min, and the mixed solution was measured at 540 nm with a spectrophotometer. To determine the optima of both pH and temperature, sodium acetate was used as the substrate. Phosphate buffer (10 mM), having a pH of 4.0 to 8.0, was used to provide different pH conditions for the enzyme reaction. When analyzing the temperature distribution, the optimum pH of each ACS was used. All mixtures were held at each temperature for 10 min before the start of the reaction. The protein activity was determined by the above method at 4, 10, 20, 30, 35, 37, 40, 50, and 55 °C temperatures.

2.8. Transcription of Pt4CL-Like in Various Tissues

Total RNA was isolated from mature and young leaves, upper and lower stems, petioles, and roots of *P. trichocarpa*, according to the reagent manufacturer's instructions. qRT-PCR was performed with a Real-Time PCR System (Applied Biosystems, Carlsbad, California, USA) using the PrimeScript RT Reagent Kit with gDNA Eraser (Takara, Dalian, China) and the SYBR Green PCR Kit (Takara, Dalian, China). qRT-PCR primers were designed for *Pt4CL-like* (Table 1), and the housekeeping gene actin was used as an internal control. qRT-PCR was carried out as follows: initial incubation at 95 °C for 5 min, followed by 40 cycles of 45 s at 95 °C, 45 s at the annealing temperature of 60 °C, and 45 s at 72 °C and, then, a final incubation for 10 min at 72 °C. Triplicate measurements were used to determine the values for each parameter, and each data point represented the mean of the measurements. The treatments for analyses of transcription of *Pt4CL-like* in various tissues were repeated three times.

2.9. Expression of Pt4CL-Like in Response to Abiotic Stress Treatments

Populus trichocarpa seedlings treated with 200 mM NaCl, 200 µm abscisic acid (ABA), or 2 mM hydrogen peroxide (H_2O_2) were sampled at 0, 2, 4, 6, 8, 12, 24, and 48 h, and those subjected to 4 °C cold stress or 10% PEG_{6000} were collected after 1, 2, 3, 4, 5, 6, and 7 days. Following treatment, RNA was extracted from poplar leaves according to the above method. Subsequently, qRT-PCR was performed as described above. Triplicate measurements were used to determine the values for each parameter, and each data point represented the mean of these measurements. The experiments of expression of *Pt4CL-like* in response to abiotic stress treatments were repeated three times.

3. Results

3.1. Molecular Cloning and Sequence Analyses of Pt4CL-Like

Full-length cDNA of *Pt4CL-like* was isolated from *P. trichocarpa*, referring to *Pt4CL-like* (XP_002307770.2). The *Pt4CL-like* ORF is 1665 base pairs (bp) in length, and encodes a peptide of 554 amino acids. Based on the sequence of *Pt4CL-like*, we designed specific primers and achieved full-length amplification of *Pt4CL-like* using RACE. The full gene length, ORF size, amino acid sequence length, MW, and pI of *Pt4CL-like* deduced protein are shown in Table 2. The deduced amino acid sequence of *Pt4CL-like* showed a high degree of homology with ACS sequences from other plant species, e.g., *Ricinus communis* (XP_017975597.1, 80.87% identity), *Durio zibethinus* (XP_007225144.1, 79.78% identity), *Gossypium arboreum* (AMJ39459, 78.88% identity), and *Corchorus olitorius* (CAD22530.1, 73.29% identity) (Figure 1). Generally speaking, the box I and box II domains of 4CL were completely conserved, according to the sequence alignment and analyses of Martínez-Blanco et al. [20], whereas the box I domain of the 4CL-like gene was relatively conserved, and the box II domain was generally

not conserved. At4CL1 (NP_001077697.1), At4CL2 (AF_106086.1), At4CL3 (AF_106087.1), Pt4CL1 (XP_002297699.20, Pt4CL4 (XP_002324477.2), and Pt4CL5 (XP_002304825.2) were chosen to identify conserved sequences. The box I domain (SSGTTGLPKGV) and the box II domain (GEICIRG) were conserved according to the sequence alignment (Figure 2A,B), but the box I domain and the box II domain were not conserved compared to sequences from *Populus trichocarpa* (XP_002307770.2), *Hevea brasiliensis* (XP_021666022.1), *Jatropha curcas* (XP_012073683.1), *Manihot esculenta* (XP_021601125.1), and others (Figure 2C,D). For example, the main differences in *Pt4CL-like* were changes in proline to serine, and leucine to glutamate, in box I. Leucine is a nonpolar amino acid, while glutamate is a polar and negatively charged amino acid; similarly, proline is a nonpolar amino acid, while serine is a polar amino acid. Changes were also observed in the box II domain, with isoleucine changing to leucine and cysteine changing to tryptophan. Tryptophan is a nonpolar amino acid, while cysteine is a polar and uncharged amino acid (Figure 2 and Figure S1).

Table 2. Length, open reading frame (ORF), amino acid sequence length, molecular weight, and predicted isoelectric points (pI) of *Pt4CL-like* deduced protein are shown.

Gene Name	Full Length(bp)	ORF (bp)	Amino Acid Sequence (aa)	Molecular Weight	pI
Pt4CL-like	2127	1665	554	60.33	7.6

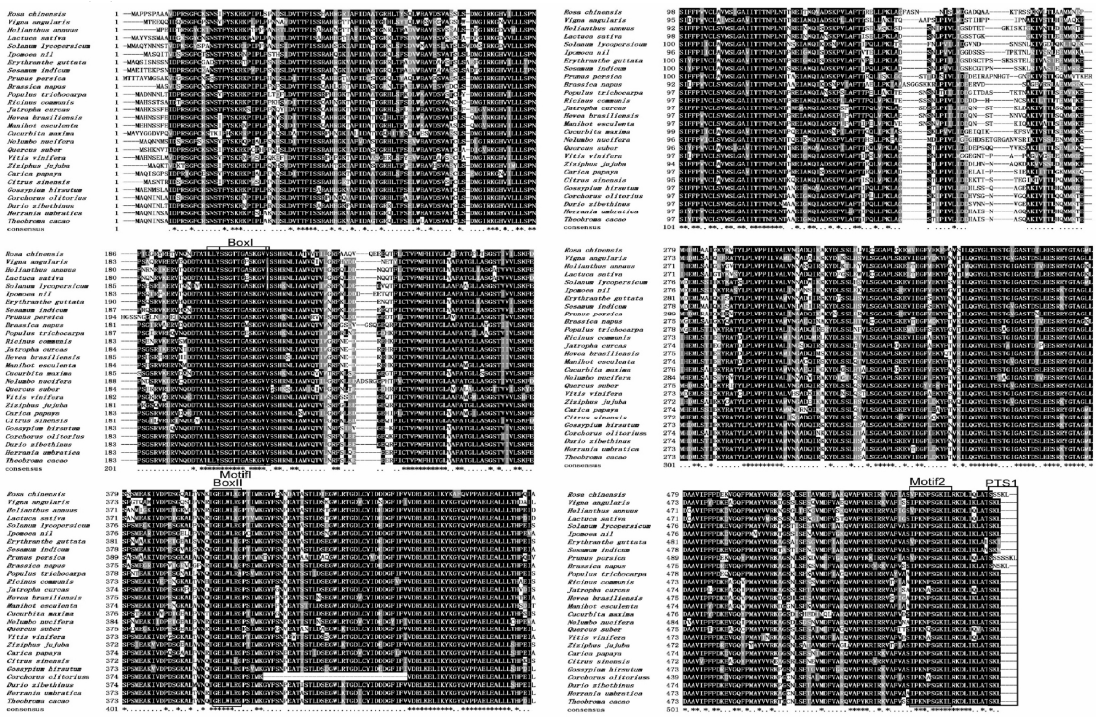

Figure 1. Comparison of the deduced amino acid sequences of conserved regions of *Populus trichocarpa*. *Pt4CL-like* and the corresponding sequences of other known AMP-forming acetyl-CoA synthetase (ACS) proteins, including *Gossypium arboreum* (XP 017613221.1), *Corchorus olitorius* (OMO85482.1), *Durio zibethinus* (XP 022772588.1), and *Ricinus communis* (XP 002510640.1) are shown. Two domains, box I and box II, are numbered and indicated by a box. A putative peroxisome targeting sequence (PTS0) is also numbered and indicated by a box.

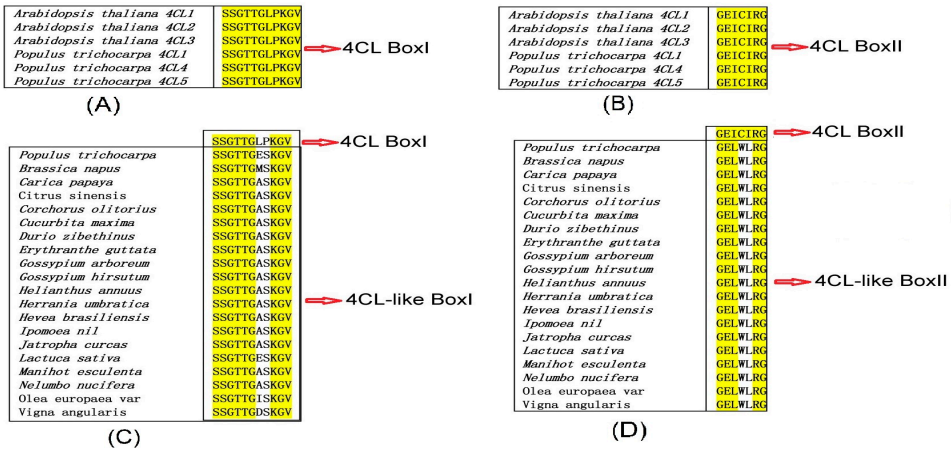

Figure 2. Comparison of the conserved regions of the box I and box II domains. (**A**) Comparison of the conserved regions of the box I domain among At4CL1 (NP_001077697.1), At4CL2 (AF_106086.1), At4CL3 (AF_106087.1), Pt4CL1 (XP_002297699.2), Pt4CL4 (XP_002324477.2), and Pt4CL5 (XP_002304825.2). (**B**) Comparison of the conserved regions of the box II domain among At4CL1, At4CL2, At4CL3, Pt4CL1, Pt4CL4, and Pt4CL5. (**C**) Comparison of the conserved regions of the box I domain among *Populus trichocarpa* (XP_002307770.2), *Brassica napus* (XP_013727429.1), *Carica papaya* (XP_021902472.1), *Citrus sinensis* (XP_006473755.1), *Corchorus olitorius* (OMO85482.1), *Cucurbita maxima* (XP_022975900.1), *Cucurbita moschata* (XP_022941144.1), *Durio zibethinus* (XP_022772588.1), *Erythranthe guttata* (XP_012829565.1), *Gossypium arboreum* (XP_017613221.1), *Gossypium hirsutum* (XP_016741834.1), *Helianthus annuus* (XP_021997613.1), *Hevea brasiliensis* (XP_021666022.1), *Jatropha curcas* (XP_012073683.1), *Ipomoea nil* (XP_019173698.1), *Manihot esculenta* (XP_021601125.1), *Lactuca sativa* (XP_023748526.1), *Nelumbo nucifera* (XP_010242836.1), *Olea europaea* var. *sylvestris* (XP_022894414.1), and *Vigna angularis* (XP_017430152.1). (**D**) Comparison of the conserved regions of the box II domain among *Populus trichocarpa* (XP_002307770.2), *Brassica napus* (XP_013727429.1), *Carica papaya* (XP_021902472.1), *Citrus sinensis* (XP_006473755.1), *Corchorus olitorius* (OMO85482.1), *Cucurbita maxima* (XP_022975900.1), *Cucurbita moschata* (XP_022941144.1), *Durio zibethinus* (XP_022772588.1), *Erythranthe guttata* (XP_012829565.1), *Gossypium arboreum* (XP_017613221.1), *Gossypium hirsutum* (XP_016741834.1), *Helianthus annuus* (XP_021997613.1), *Hevea brasiliensis* (XP_021666022.1), *Jatropha curcas* (XP_012073683.1), *Ipomoea nil* (XP_019173698.1), *Manihot esculenta* (XP_021601125.1), *Lactuca sativa* (XP_023748526.1), *Nelumbo nucifera* (XP_010242836.1), *Olea europaea* var. *sylvestris* (XP_022894414.1), and *Vigna angularis* (XP_017430152.1).

Changes in the polarity of amino acids may lead to changes in protein properties, and, therefore, we speculate that *Pt4CL-like* may have the different catalytic activity to 4CL [21,22].

3.2. 3D Structure and Phylogenetic Analyses

Modeling of 3D structures was conducted using the SWISS-MODEL server, and the 3D structures of Pt4CL1, Pt4CL4, Pt4CL5, At4CL1, At4CL2, and At4CL3 were predicted. Furthermore, 4CL-like proteins from *Populus trichocarpa*, *Hevea brasiliensis*, *Jatropha curcas*, and *Manihot esculenta* were also predicted. Structure comparison was used to identify similarities among protein sequences, and the results indicated that the box I domain of Pt4CL1, Pt4CL4, Pt4CL5, At4CL1, At4CL2, and At4CL3 was a conserved sequence, as was the box II domain of Pt4CL1, Pt4CL4, Pt4CL5, At4CL1, At4CL2, and At4CL3 (Figure S2A,B). However, the box I and box II domains of 4CL-like proteins were not conserved, and only the conserved PTS sequence was observed to have C-terminal modification (Figure S2C). For investigating the evolutionary relationships between the 4CL-like protein and other adenylate-forming enzymes, we performed phylogenetic analysis using the MEGA 5.0 program. The phylogenetic analysis results illustrated that 4CL-like had high homology with other amino acid sequences from ACS, and 4CL-like

protein was most closely related to evolution of other ACS protein sequences, such as those from *Manihot esculenta* (XP_021601125.1) and *Jatropha curcas* (XP_012073683.1) (Figure 3).

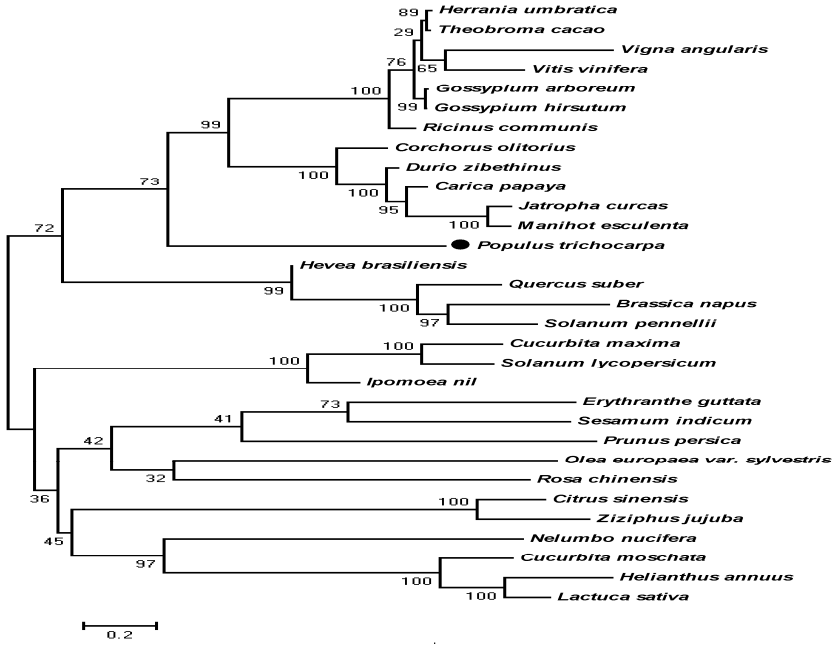

Figure 3. Phylogenetic tree showing the relationships between the *Pt4CL-like* (XP_002307770.2) amino acid sequence and other identified 4CL-like sequences. The tree was constructed using the neighbor-joining (NJ) method in MEGA 5.1 and bootstrapped 1000 times. Bootstrap percentages are indicated at the branch points. In all cases, tree topologies obtained using the NJ, minimum evolution, and maximum parsimony methods were identical. Accession numbers of *Def* sequences obtained from GenBank are as follows: *Brassica napus* (XP_013727429.1), *Carica papaya* (XP_021902472.1), *Citrus sinensis* (XP_006473755.1), *Corchorus olitorius* (OMO85482.1), *Cucurbita maxima* (XP_022975900.1), *Cucurbita moschata* (XP_022941144.1), *Durio zibethinus* (XP_022772588.1), *Erythranthe guttata* (XP_012829565.1), *Gossypium arboreum* (XP_017613221.1), *Gossypium hirsutum* (XP_016741834.1), *Helianthus annuus* (XP_021997613.1), *Hevea brasiliensis* (XP_021666022.1), *Ipomoea nil* (XP_019173698.1), *Jatropha curcas* (XP_012073683.1), *Lactuca sativa* (XP_023748526.1), *Manihot esculenta* (XP_021601125.1), *Nelumbo nucifera* (XP_010242836.1), *Olea europaea var. sylvestris* (XP_022894414.1), *Populus trichocarpa* (XP_002307770.2), *Prunus persica* (XP_007222465.1), *Quercus suber* (XP_023922725.1), *Ricinus communis* (XP_002510640.1), *Sesamum indicum* (XP_011099557.1), *Solanum lycopersicum* (XP_004253129.1), *Solanum pennellii* (XP_015059189.1), *Theobroma cacao* (XP_007017972.2), *Vigna angularis* (XP_017430152.1), *Vitis vinifera* (XP_002285920.1), and *Ziziphus jujuba* (XP_015884135.1).

3.3. Prokaryotic Expression, Purification, and Western Blot

The vector pET28a was used as an expression vector, and the ORF of the 4CL-like gene of *P. trichocarpa* was inserted into this prokaryotic vector between the *Not*I and *Nde*I restriction sites (Figure 4A). Then, the recombinant plasmid pET28a-*Pt4CL-like* was transformed to *E. coli* strain BL21 and the recombinant expression bacteria were obtained. After induction with 1 mM IPTG for 4 h, the *Pt4CL-like* protein was expressed (Figure 4B), and analyses of the supernatant and precipitate indicated that the recombinant protein was present in the form of inclusion bodies (Figure 4C). To identify the influence of IPTG concentration, temperature, and shaking speed on protein expression, treatments of 0.3, 0.5, and 1 mM IPTG, at 16 and 37 °C, and at 110 and 220 rpm, were carried out. Through the analysis of different concentrations of IPTG, different induction temperatures and different induction speed, we found that the *Pt4CL-like* protein always exists in the precipitate, and no target protein was detected in the supernatant when the recombinant bacteria were induced to express protein using low concentrations of IPTG, low induction temperatures and low induction speeds, so we had to carry out denaturation and renaturation of the protein (Figure 4D).

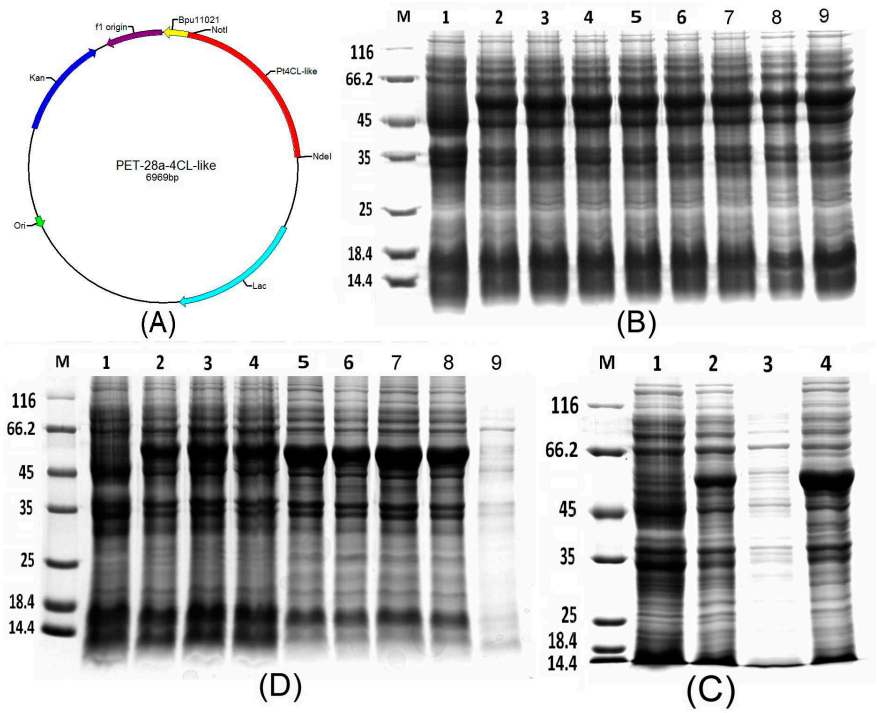

Figure 4. Construction of the prokaryotic expression vector for PET-28a-*Pt4CL-like* and analyses of the expressed fusion protein through 12% polyacrylamide gel electrophoresis (SDS-PAGE). (**A**) Construction of the prokaryotic expression vector for PET-28a-*Pt4CL-like*, using *Nde*I and *Not*I as the two restriction enzymes. (**B**) Analyses of the expressed fusion protein through 12% SDS-PAGE. Lane M: molecular mass marker; lane 1: negative control; lanes 2–9: colonies 1–8, respectively, induced with 1 mM isopropyl β-D-1-thiogalactopyranoside (IPTG). The molecular weight of the target protein was about 57 kDa, indicated by the black arrow. (**C**) Supernatant and precipitate analyses via 12% SDS-PAGE. Lane M: molecular mass marker; lane 1: negative control; lane 2: colony induced with 1 mM IPTG. Lane 3: supernatant. Lane 4: precipitate. (**D**) Analyses of the influence of IPTG concentration, temperature and shaking speed on protein expression. Lane M: molecular mass marker; lane 2: *Pt4CL-like* protein induced with 0.3 mM IPTG at 37 °C and 220 rpm for 4 h; lane 3: *Pt4CL-like* protein induced with 0.5 mM IPTG at 37 °C and 220 rpm for 4 h; lane 4: *Pt4CL-like* protein induced with 1 mM IPTG at 37 °C and 220 rpm for 4 h; lane 5: *Pt4CL-like* protein induced with 0.5 mM IPTG at 16 °C and 100 rpm for 10 h; lane 6: precipitate achieved from bacteria induced with 0.5 mM IPTG at 16 °C and 100 rpm for 10 h; lane 7: *Pt4CL-like* protein induced with 0.5 mM IPTG at 16 °C and 100 rpm for 16 h; lane 8: precipitate achieved from bacteria induced with 0.5 mM IPTG at 16 °C and 100 rpm for 16 h; lane 9: supernatant achieved from bacteria induced with 0.5 mM IPTG at 16 °C and 100 rpm for 10 h.

The targeted protein was expressed in the precipitate according to 12% SDS-PAGE analyses and, thus, was considered an inclusion body. Therefore, manipulation of denaturation and renaturation conditions was carried out to focus on inclusion bodies. The inclusion body could not be released when 2 M urea and 4 M urea was used to manipulate the precipitate (Figure 5A). A small amount of the inclusion body was released when 6 M urea was used to treat the precipitate (Figure 5A). When 8 M urea was used, the inclusion body could be released according to 12% SDS-PAGE (Figure 5A). The entire denaturation process is shown in Figure 6 (Left). The inclusion body that was released had no biological activity and, therefore, the process of renaturation was carried out in vitro to restore protein activity. The entire renaturation process is shown in Figure 6 (Right).

HisTrap HP affinity chromatography was used to purify the recombinant *Pt4CL-like* protein. His-tagged proteins were captured using Ni-IDA resin, washed repeatedly in a buffer containing 20 mM imidazole, and eluted in a buffer containing 250 mM imidazole (Figure 5C). The *Pt4CL-like* protein fraction was eluted with 250 mM imidazole, as shown in 12% SDS-PAGE analyses (Figure 5B),

and a pure band of 60 kDa was observed, in agreement with the theoretical mass of *Pt4CL-like* protein (57 kDa) with the His tag protein. Western blotting was used to determine whether *Pt4CL-like* protein could be specifically recognized by rabbit antiserum against His-*Pt4CL-like* expressed in *E. coli* BL21 (DE3). The rabbit antiserum successfully identified His-*Pt4CL-like*, confirming that the peptides expressed by BL21 (DE3) were *Pt4CL-like* protein (Figure 5B).

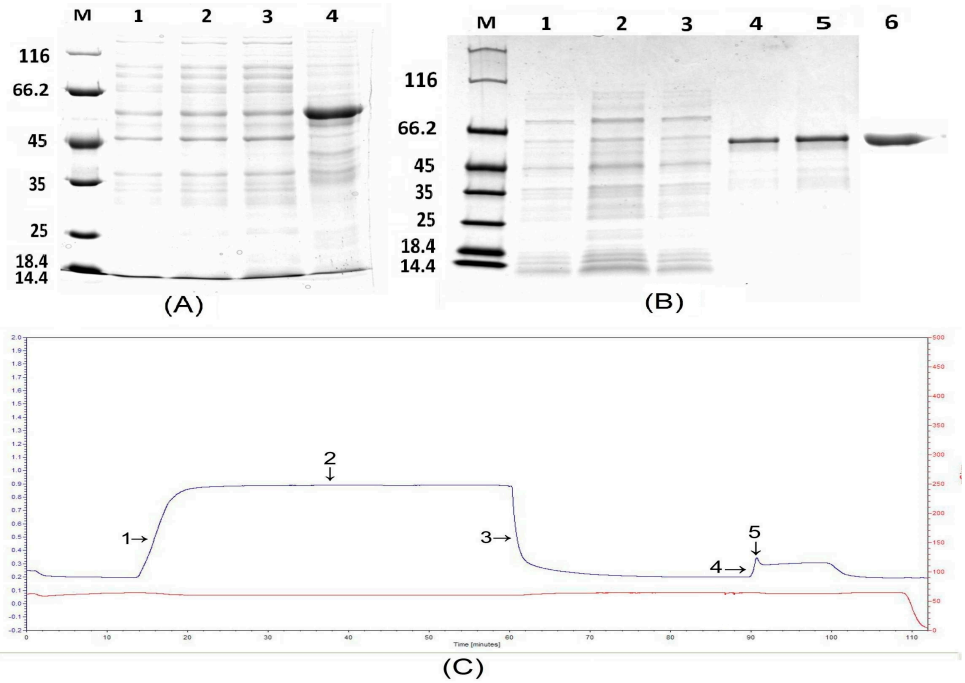

Figure 5. The process of denaturation and purification of the *Pt4CL-like* protein. (**A**) The denaturation process of *Pt4CL-like* protein. Lane M: molecular mass marker; lane 1: denaturation with 2 M urea; lane 2: denaturation with 4 M urea; lane 3: denaturation with 6 M urea; lane 4: denaturation with 8 M urea; (**B**) Purification of the *Pt4CL-like* fusion protein. Lane M: molecular weight marker; lane 1–2: flow-through; lane 3: wash; lane 4–5: elution; lane 6: Western blotting analyses of purified *Pt4CL-like* fusion protein using a mAb against the His6 tag. (**C**) Ni-IDA affinity chromatography of the fusion protein carried out using LP Data View software (Biologic LP, Bio-rad, Hercules, USA).

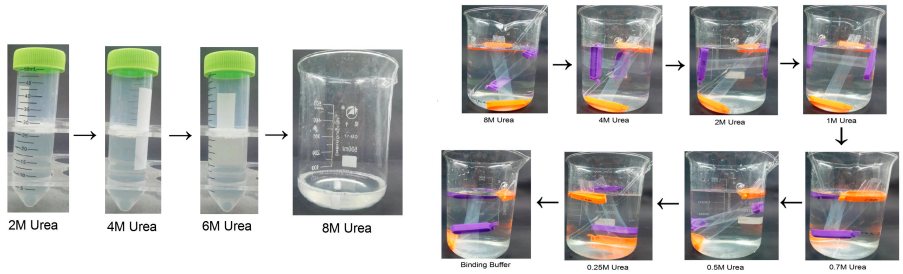

Figure 6. (**A**) Image of the denaturation process. 1: Inclusion body dissolved 3 times in 2 M urea. 2: Inclusion body dissolved 2 times in 4 M urea. 3: Inclusion body dissolved once in 6 M urea. 4: Inclusion body dissolved in 8 M urea was placed in a refrigerator at 4 °C overnight. (**B**) Image of the renaturation process. Renaturation buffer (4–0.5 M urea, 0.5 M NaCl, 10 mM Tris, 0.5 mM ethylenediaminetetraacetic acid(EDTA), 1 mM L-arginine, 1 mM reduced L-glutathione, 0.2 mM oxidized L-glutathione, and 5 mM DL-Dithiothreitol (DTT), pH 8.5) was gradually added in a series of four dilutions and slowly stirred until the concentration of urea reached 0.25 M. The protein solution was transferred to a dialysis bag and incubated overnight at 4 °C in dialysis buffer. During dialysis, the concentration was reduced, and binding buffer (20 mM Tris-base, 500 mM NaCl, and 20 mM imidazole) was used as the final dialysis buffer.

3.4. Enzymatic Activity of Pt4CL-Like Protein and Effects of pH and Temperature on its Activity

To further identify the enzymatic characteristics of recombinant *Pt4CL-like* protein, substrate specificity was examined. Generally, when the substrate was ferulate acid, 4-coumaric acid ester, and caffeate, 4CLs exhibited higher activity. However, when the substrate was sodium acetate, ACS showed higher activity (7, 16). To determine the activity of recombinant *Pt4CL-like* proteins, different substrates, including sodium acetate, coumaric acid, caffeic acid, and ferulic acid, were selected for this study. The results showed that the recombinant *Pt4CL-like* protein can catalyze sodium acetate, but has no catalytic ability to coumaric acid, caffeic acid and ferulic acid (Table 3). Also, we constructed the Michaelis-Menten equation and calculated a Michaelis constant (K_m) of 1.91 ± 0.05 and V_{max} of 1.26 ± 0.075 (Table 3).

Table 3. Different substrates' K_m and V_{max}.

Enzyme	Substrate	K_m (mmol/Ls)	V_{max} (mmol/Ls)
Pt4CL-like protein	coumarate	-	-
	caffeate	-	-
	ferulate	-	-
	sodium acetate	1.91 ± 0.050	1.26 ± 0.075

Next, the effects of pH on enzyme activity were evaluated. The activity of recombinant *Pt4CL-like* protein was pH-dependent. Recombinant *Pt4CL-like* protein showed high levels of activity in the pH range of 6.0–7.0, with a pH optimum of 7.0. Little activity was detected at pH levels below 5.0 or above 8.0 (Figure 7A). Temperature profile analyses indicated that a temperature of 37 °C was optimum for enzymatic activity (Figure 7B); its activity decreased sharply at 40 °C–50 °C.

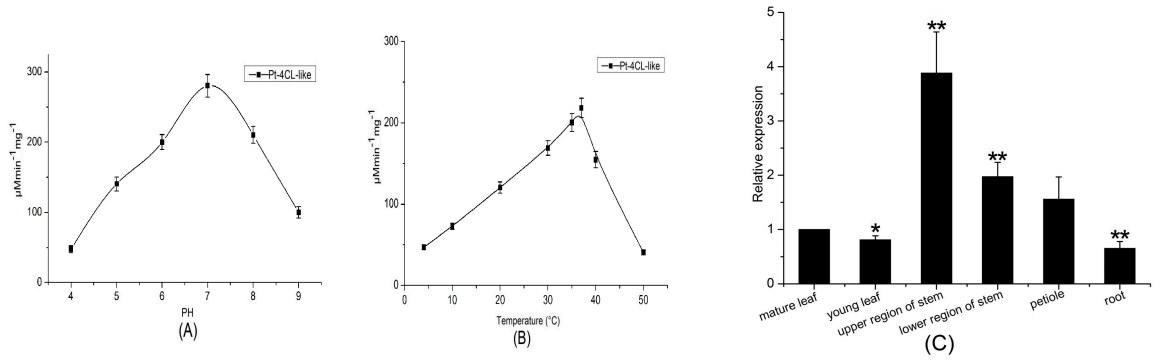

Figure 7. Biological activities of the purified *Pt4CL-like* enzyme. (**A**) Catalytic activity of recombinant *Pt4CL-like* enzyme under different pH conditions. (**B**) Catalytic activity of recombinant *Pt4CL-like* enzyme under different temperature conditions. (**C**) Expression analyses of the *Pt4CL-like* gene in various tissues. Mean levels (including standard deviations; SD) in six tissues were analyzed via real-time qPCR. Data are $2^{-\Delta\Delta Ct}$ levels calculated relative to the reference tissue (root), which was set to 1, and normalized to actin mRNA levels. Vertical bars represent mean ± SD (n = 3). Asterisk indicates a significant difference at $p < 0.05$. Double asterisk indicates a significant difference at $p < 0.01$.

3.5. Analyses of Tissue-Specific Expression of the Pt4CL-Like Gene and Transcript Levels of Pt4CL-Like Gene Following Induction with 200 mM NaCl, 200 μM ABA, 2 mM H_2O_2, 4 °C Cold Stress, and 10% PEG_{6000}

Quantitative real-time PCR was used to investigate the expression profile of the *Pt4CL-like* gene in various tissues (mature and young leaves, upper and lower stems, petioles, and roots); the gene-specific primers used are shown in Table 1. Transcription levels of *Pt4CL-like* gene were high in the upper and lower regions of stems, while the lowest expression level was observed in roots, with an almost 4-fold higher expression in young leaves than in roots (Figure 7C).

To identify the transcription pattern of the *Pt4CL-like* gene under stress, *P. trichocarpa* seedlings were subjected to the following abiotic stresses: 200 mM NaCl, 200 μM ABA, 2 mM H_2O_2, 4 °C cold stress, and 10% PEG_{6000}. The expression of *Pt4CL-like* was altered to varying degrees in response to these treatments. The highest level of *Pt4CL-like* gene expression was observed after 12 h of treatment with 200 μM ABA, which was approximately 5.5 times that of the control and was followed by a gradual decline (Figure 8A). Following treatment with 10% PEG_{6000} for 7 days, *Pt4CL-like* gene transcription was upregulated approximately 1.8-fold compared to the control, which was also followed by a gradual decline (Figure 8C). Expression of *Pt4CL-like* was enhanced with 1–48 h of 200 mM NaCl treatment, and the maximum difference in expression occurred at 12 h (Figure 8B). Following treatment with the abiotic stressor 2 mM H_2O_2, the expression of the *Pt4CL-like* gene was upregulated, reaching a level approximately 1.7-fold higher than the control at 24 h (Figure 8E). *Pt4CL-like* gene expression was induced by cold stress of 4 °C (control temperature, 23 °C) and reached a maximum level of expression after 7 days of treatment (Figure 8D).

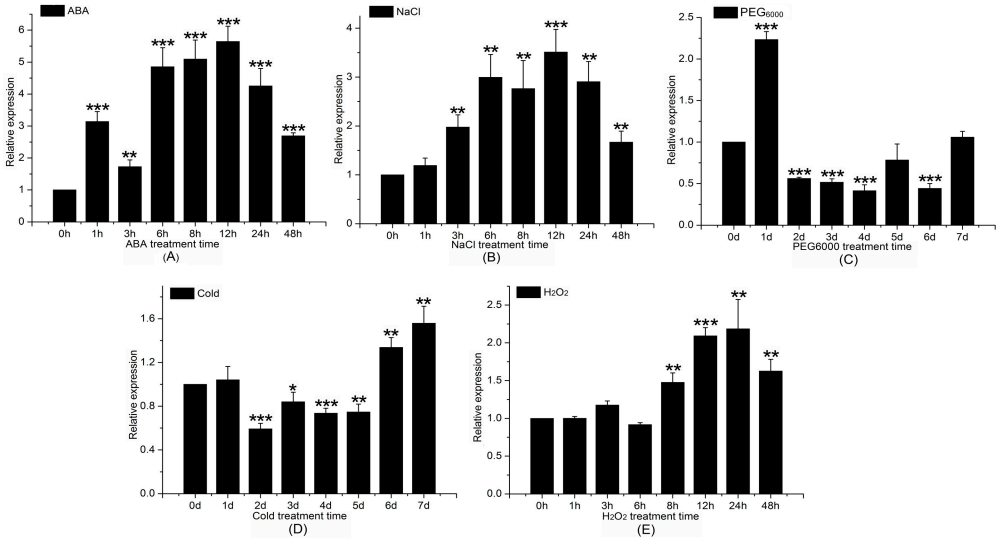

Figure 8. Expression time series of *Pt4CL-like* gene in response to different stress treatments, as determined via qPCR. qPCR was performed with total RNA extracted from leaves at the indicated times after treatment with 200 μM abscisic acid (ABA) (**A**), 200 mM NaCl (**B**), 10% PEG_{6000} (**C**), 4 °C cold stress (**D**), and 2 mM hydrogen peroxide (H_2O_2) (**E**). Relative expression was calculated using actin as an internal reference. Leaves treated with distilled water under the same conditions served as controls. Vertical bars represent mean ± SD (n = 3). Three independent experiments were performed. Asterisk indicates a significant difference at $p < 0.05$. Double asterisk indicates a significant difference at $p < 0.01$.

4. Discussion

4CL plays a significant role in the phenylpropanoid pathway, as it can catalyze the formation of hydroxycinnamoyl-CoA thioesters, precursors for the synthesis of lignins, monolignols, flavonoids, stilbenes, coumarins, and other phenylpropanoids. Previous studies of 4CL genes have focused on their key roles in biosynthetic pathways of lignins, monolignols, and flavonoids [22–25], but few 4CL-like genes have been identified, and little is known about their characteristics and functions [15,18].

Generally speaking, through the enzymatic reaction of ACS, acetate and ATP are converted to an acetyl adenylate intermediate, and the acetyl moiety is transferred to CoA to form acetyl-CoA [16,26,27]. It is very hard to confirm the relationship between the ACS and 4CL groups due to the high similarity of their protein structures. In this study, cDNA of the *Pt4CL-like* gene was isolated, and the *Pt4CL-like* protein was expressed and purified in *E. coli*. *Pt4CL-like* was highly conserved with ACSs from other species and had a close relationship with ACSs from *Ricinus communis* (XP_017975597), *Durio zibethinus* (XP_007225144.1), *Gossypium arboreum* (AMJ39459), and *Corchorus olitorius* (CAD22530.1).

Moreover, unlike the box I and box II domains of the Pt4CL gene, the box I domain of *Pt4CL-like* was relatively conserved, and its box II domain was generally not conserved. The main differences were changes in proline to serine and leucine to glutamate in box I. Leucine is a nonpolar amino acid, but glutamate is polar and negatively charged; similarly, proline is a nonpolar amino acid, but serine is a polar amino acid. Changes also occur in the box II domain, where isoleucine changes to leucine, and cysteine to tryptophan. Tryptophan is a nonpolar amino acid, while cysteine is polar and uncharged (Figure 2). Changes in the polarity of amino acids may lead to changes in protein properties and, therefore, we speculated that *Pt4CL-like* may exhibit the different catalytic activity with 4CL [16,28]. In addition, phylogenetic analyses revealed that *Pt4CL-like* had a closer relationship with ACSs from *Manihot esculenta* (XP_021601125.1) and *Jatropha curcas* (XP_012073683.1) and, thus, that *Pt4CL-like* belongs to the ACS family. In the whole genome of *Arabidopsis*, nine adenylate synthetase genes have been found and classified as 4CL-like genes [1], and these genes exhibit very high similarity, in the substrate-binding region and the conserved region, with true 4CL genes [22]. Unlike 4CL proteins, the 4CL-like proteins are predicted to play a role in the synthesis of peroxisomes due to the presence of peroxisome sequences (PTS) at the C-terminal end of 4CL-like proteins. In this study, the *Pt4CL-like* protein investigated (XP_002307770.2) also has PTS at its C-terminal end and, thus, may target the peroxisome.

For characterization and functional analyses of the 4CL-like gene from *Populus trichocarpa*, its enzymatic activity was observed. The recombinant 4CL-like protein had no reaction with the substrates of 4CL, but reacted with sodium acetate, which indicates that *Pt4CL-like* belongs to the ACS family. Compared to phylogenetic analyses and structure prediction, enzymatic analyses could represent a more effective method for characterizing 4CL-like proteins. The methods we used for characterization and functional analyses of the 4CL-like gene have been used in *Dunaliella tertiolecta* and *Mycobacterium tuberculosis* [29,30]. Previous research has shown that lipid contents in *D. tertiolecta* increase under conditions of nitrogen deficiency, and cells cultivated in nitrogen-deficient medium accumulate the greatest amounts of lipid [24]. In our study, *Pt4CL-like* responded to various abiotic stressors, including high salinity, low temperature, and drought. Our results suggest that 4CL-like activity in *Populus trichocarpa* may be related to abiotic stress. In addition, we analyzed tissue-specific expression of the *Pt4CL-like* gene, and found that it has high transcriptional levels in the upper and lower regions of stems and the lowest expression level in roots. We predict that *Pt4CL-like* may play essential roles in plant development and environmental interactions.

In conclusion, the cDNA of 4CL-like from *Populus trichocarpa* was isolated, and the 4CL-like protein was purified. We found that 4CL-like showed enzymatic activity, and could be classified into the ACS family. In addition, a higher transcript level of *Pt4CL-like* gene was determined in stems, and *Pt4CL-like* gene can respond to a variety of stresses, which suggests that this protein is involved in plant development and environmental interactions.

Supplementary Materials: Supplementary Materials are available online at http://www.mdpi.com/2227-9717/7/1/45/s1. Figure S1. Image of the predicted tertiary structure of 4CL and 4CL-like proteins. the α-helices are represented in yellow, the β-strands are represented in purple, and random coils are represented in blue. For special domains, box I is highlighted in red and box II is highlighted in green. (A) Tertiary structure prediction of Pt4CL1. (B) Tertiary structure prediction of Pt4CL4. (C) Tertiary structure prediction ofPt4CL5. (D) Tertiary structure prediction of At4CL1. (E) Tertiary structure prediction of At4CL2. (E) Tertiary structure prediction of At4CL3. (G) Tertiary structure prediction of *Pt4CL-like*. (H) Tertiary structure prediction of ACS from *Hevea brasiliensis* (XP_021666022.1). (I) Tertiary structure prediction of ACS from *Jatropha curcas* (XP_012073683.1). (J) Tertiary structure prediction of ACS from *Manihot esculenta* (XP_021601125.1); Figure S2. Structure comparison of the predicted tertiary structures of Pt4CL1, Pt4CL4, Pt4CL5, At4CL1, At4CL2, At4CL3 and 4CL-like proteins. In the image representation, the α-helices are represented in yellow, the β-strands are represented in purple, and random coils are represented in blue (A) Structure comparison of the predicted tertiary structure of Pt4CL proteins. For special domains, box I is highlighted in red and box II is highlighted in green. (B) Structure comparison of the predicted tertiary structures of At4CL proteins. For special domains, box I is highlighted in red and box II in green. (C) Structure comparison of the predicted tertiary structure of 4CL-like proteins from *Populus trichocarpa* (XP_002307770.2), *Hevea brasiliensis* (XP_021666022.1), *Jatropha curcas* (XP_012073683.1), and *Manihot esculenta* (XP_021601125.1). The special domain of the PTS sequence is highlighted in black.

Author Contributions: H.W. and A.M. designed and write the manuscript. H.W., A.M., C.X. and W.S. performed experiments. Q.Z. supervised this research.

Funding: This work was supported by the National Science Foundation of China (No. 31570650), and the Priority Academic Program Development of Jiangsu Higher Education Institutions.

Acknowledgments: We like to thank all students in Key Laboratory of Forest Genetics & Biotechnology that help us to perform experiments well.

Conflicts of Interest: The authors declare no conflicts of interest.

References

1. Schneider, K.; Kienow, L.; Schmelzer, E.; Colby, T.; Bartsch, M.; Miersch, O.; Wasternack, C.; Kombrink, E.; Stuible, H.P. A new type of peroxisomal acyl-coenzyme A synthetase from *Arabidopsis thaliana* has the catalytic capacity to activate biosynthetic precursors of jasmonic acid. *J. Biol. Chem.* **2005**, *280*, 13962–13972. [CrossRef]
2. Starai, V.; Escalante-Semerena, J. Acetyl-coenzyme A synthetase (AMP forming). *Cell. Mol. Life Sci.* **2004**, *61*, 2020–2030. [CrossRef] [PubMed]
3. Mai, X.; Adams, M. Purification and characterization of two reversible and ADP-dependent acetyl coenzyme A synthetases from the hyperthermophilic archaeon *Pyrococcus furiosus*. *J. Bacteriol.* **1996**, *178*, 5897–5903. [CrossRef] [PubMed]
4. Sanchez, L.B.; Morrison, H.G.; Sogin, M.L.; Muller, M. Cloning and sequencing of an acetyl-CoA synthetase (ADP-forming) gene from the amitochondriate protist, *Giardia lamblia*. *Gene* **1999**, *233*, 225–231. [CrossRef]
5. Stuible, H.P.; Kombrink, E. Identification of the substrate specificity-conferring amino acid residues of 4-coumarate: Coenzyme A ligase allows the rational design of mutant enzymes with new catalytic properties. *J. Biol. Chem.* **2001**, *276*, 26893–26897. [CrossRef]
6. Weisshaar, B.; Jenkins, G.I. Phenylpropanoid biosynthesis and its regulation. *Curr. Opin. Plant Biol.* **1998**, *1*, 251–257. [CrossRef]
7. Hamberger, B.; Hahlbrock, K. The 4-coumarate:CoA ligase gene family in *Arabidopsis thaliana* comprises one rare, sinapate-activating and three commonly occurring isoenzymes. *Proc. Natl. Acad. Sci. USA* **2004**, *101*, 2209–2214. [CrossRef] [PubMed]
8. Li, R.; Gu, J.; Chen, P.; Zhang, Z.; Deng, J.; Zhang, X. Purification and characterization of the acetyl-CoA synthetase from *Mycobacterium tuberculosis*. *Acta Biochim. Biophys. Sin.* **2015**, *43*, 891–899. [CrossRef]
9. Hu, W.J.; Kawaoka, A.; Tsai, C.J.; Lung, J.; Osakabe, K.; Ebinuma, H.; Chiang, V.L. Compartmentalized expression of two structurally and functionally distinct 4-coumarate: CoA ligase genes in aspen (*Populus tremuloides*). *Proc. Natl. Acad. Sci. USA* **1998**, *95*, 5407–5412. [CrossRef]
10. Shi, R.; Sun, Y.H.; Li, Q.; Heber, S.; Sederoff, R.; Chiang, V.L. Towards a systems approach for lignin biosynthesis in *Populus trichocarpa*: Transcript abundance and specificity of the monolignol biosynthetic genes. *Plant Cell Physiol.* **2010**, *51*, 144–163. [CrossRef]
11. Chen, H.-C.; Song, J.; Williams, C.M.; Shuford, C.M.; Liu, J.; Wang, J.P.; Li, Q.; Shi, R.; Gokce, E.; Ducoste, J.; et al. Monolignol pathway 4-coumaric acid: Coenzyme A ligases in *Populus trichocarpa*: Novel specificity, metabolic regulation, and simulation of coenzyme A ligation fluxes. *Plant Physiol.* **2013**, *161*, 1501–1516. [CrossRef]
12. Ehlting, J.; Buttner, D.; Wang, Q.; Douglas, C.J.; Somssich, I.E.; Kombrink, E. Three 4-coumarate:coenzyme A ligases in *Arabidopsis thaliana* represent two evolutionarily divergent classes in angiosperms. *Plant J.* **2010**, *19*, 9–20. [CrossRef]
13. Raes, J.; Rohde, A.; Christensen, J.H.; Van de Peer, Y.; Boerjan, W. Genome-wide characterization of the lignification toolbox in *Arabidopsis*. *Plant Physiol.* **2003**, *133*, 1051–1071. [CrossRef]
14. Ehlting, J.; Mattheus, N.; Aeschliman, D.S.; Li, E.; Hamberger, B.; Cullis, I.F.; Zhuang, J.; Kaneda, M.; Mansfield, S.D.; Samuels, L.; et al. Global transcript profiling of primary stems from *Arabidopsis thaliana* identifies candidate genes for missing links in lignin biosynthesis and transcriptional regulators of fiber differentiation. *Plant J.* **2010**, *42*, 618–640. [CrossRef]
15. Kienow, L.; Schneider, K.; Bartsch, M.; Stuible, H.-P.; Weng, H.; Miersch, O.; Wasternack, C.; Kombrink, E. Jasmonates meet fatty acids: Functional analysis of a new acyl-coenzyme A synthetase family from *Arabidopsis thaliana*. *J. Exp. Bot.* **2008**, *59*, 403–419. [CrossRef]

16. Costa, M.A.; Bedgar, D.L.; Moinuddin, S.G.; Kim, K.W.; Cardenas, C.L.; Cochrane, F.C.; Shockey, J.M.; Helms, G.L.; Amakura, Y.; Takahashi, H.; et al. Characterization in vitro and in vivo of the putative multigene 4-coumarate:CoA ligase network in *Arabidopsis*: Syringyl lignin and sinapate/sinapyl alcohol derivative formation. *Phytochemistry* **2005**, *66*, 2072–2091. [CrossRef]
17. Zhang, C.H.; Ma, T.; Luo, W.C.; Xu, J.M.; Liu, J.Q.; Wan, D.S. Identification of 4CL genes in desert poplars and their changes in expression in response to salt stress. *Genes* **2015**, *6*, 901–917. [CrossRef]
18. Koo, A.J.K.; Chung, H.S.; Kobayashi, Y.; Howe, G.A. Identification of a peroxisomal acyl-activating enzyme involved in the biosynthesis of jasmonic acid in *Arabidopsis*. *J. Biol. Chem.* **2006**, *281*, 33511–33520. [CrossRef]
19. Knobloch, K.H.; Hahlbrock, K. 4-Coumarate:CoA ligase from cell suspension cultures of *Petroselinum hortense* Hoffm. Partial purification, substrate specificity, and further properties. *Arch. Biochem. Biophys.* **1977**, *184*, 237–248. [CrossRef]
20. Martínez-Blanco, H.; Reglero, A.; Rodriguez-Aparicio, L.B.; Luengo, J.M. Purification and biochemical characterization of phenylacetyl-CoA ligase from *Pseudomonas putida*. A specific enzyme for the catabolism of phenylacetic acid. *J. Biol. Chem.* **1990**, *265*, 7084–7090.
21. Brown, T.D.; Jonesmortimer, M.C.; Kornberg, H.L. The enzymic interconversion of acetate and acetyl-coenzyme A in *Escherichia coli*. *J. Microbiol.* **1977**, *102*, 327–336. [CrossRef] [PubMed]
22. Lindermayr, C.; Mollers, B.; Fliegmann, J.; Uhlmann, A.; Lottspeich, F.; Meimberg, H.; Ebel, J. Divergent members of a soybean (*Glycine max* L.] 4-coumarate:coenzyme A ligase gene family. *Eur. J. Biochem.* **2002**, *269*, 1304–1315. [CrossRef]
23. Yang, J.; Chen, F.; Yu, O.; Beachy, R.N. Controlled silencing of 4-coumarate:CoA ligase alters lignocellulose composition without affecting stem growth. *Plant Physiol. Biochem.* **2011**, *49*, 103–109. [CrossRef] [PubMed]
24. Chen, M.; Tang, H.; Ma, H.; Holland, T.C.; Ng, K.Y.S.; Salley, S.O. Effect of nutrients on growth and lipid accumulation in the green algae *Dunaliella tertiolecta*. *Bioresour. Technol.* **2011**, *102*, 1649–1655. [CrossRef] [PubMed]
25. Sun, H.; Li, Y.; Feng, S.; Zou, W.; Guo, K.; Fan, C.; Si, S.; Peng, L. Analysis of five rice 4-coumarate: Coenzyme A ligase enzyme activity and stress response for potential roles in lignin and flavonoid biosynthesis in rice. *Biochem. Biophys. Res. Commun.* **2013**, *430*, 1151–1156. [CrossRef]
26. Shockey, J.M.; Fulda, M.S.; Browse, J. *Arabidopsis* contains a large superfamily of acyl-activating enzymes. Phylogenetic and biochemical analysis reveals a new class of acyl-coenzyme A synthetases. *Plant Physiol.* **2003**, *132*, 1065–1076. [CrossRef] [PubMed]
27. Reumann, S.; Ma, C.; Lemke, S.; Babujee, L. AraPerox. A database of putative *Arabidopsis* proteins from plant peroxisomes. *Plant Physiol.* **2004**, *136*, 2587–2608. [CrossRef]
28. Ehlting, J.; Shin, J.J.; Douglas, C.J. Identification of 4-coumarate: Coenzyme A ligase (4CL) substrate recognition domains. *Plant J. Cell. Mol. Biol.* **2010**, *27*, 455–465. [CrossRef]
29. Liang, M.-H.; Qv, X.-Y.; Jin, H.-H.; Jiang, J.-G. Characterization and expression of AMP-forming acetyl-CoA synthetase from *Dunaliella tertiolecta* and its response to nitrogen starvation stress. *Sci. Rep.* **2016**, *6*, 23445. [CrossRef]
30. Li, Y.; Kim, J.I.; Pysh, L.; Chapple, C. Four isoforms of *Arabidopsis thaliana* 4-coumarate: CoA ligase (4CL) have overlapping yet distinct roles in phenylpropanoid metabolism. *Plant Physiol.* **2015**, *169*, 2409. [CrossRef] [PubMed]